Bioimaging for Targeted Delivery of Hyaluronic Acid Derivatives to the Livers in Cirrhotic Mice Using Quantum Dots

Ki Su Kim,[†,§] Wonhee Hur,[‡,§] Sang-Jun Park,[†] Sung Woo Hong,[‡] Jung Eun Choi,[‡] Eun Ji Goh,[†] Seung Kew Yoon,[‡,*] and Sei Kwang Hahn[†,*]

[†]Department of Materials Science and Engineering, Pohang University of Science and Technology (POSTECH), San 31, Hyoja-dong, Nam-gu, Pohang, Kyungbuk 790-784, Korea, and [‡]Department of Internal Medicine and WHO Collaborating Center of Viral Hepatitis, The Catholic University of Korea, 505 Banpo-dong, Seocho-gu, Seoul 137-701, Korea. [§]These authors contributed equally to this work.

The liver is one of the most important organs in the body, with various biological and physiological functions such as filtering the blood, producing bile for the digestion and excretion of fatty substances, metabolizing many drugs, producing important proteins, like albumin, and helping break down and recycle red blood cells. Liver diseases are mainly caused by viral infections, bacterial invasion, and chemical or physical changes in the body. Among them, liver cirrhosis is an important disease with a high morbidity and mortality rate worldwide. It is characterized by the increased deposition of an extracellular matrix, including types I and III collagens, proteoglycans, fibronectin, and hyaluronic acid (HA), which results in compromised liver function.[1−4] A central phenomenon in the pathogenesis of liver fibrosis is the proliferation of hepatic stellate cells (HSC) producing an extracellular matrix in response to the injury.[5] Accordingly, they are the target cells of antifibrotic therapy. Over the past few decades, a lot of antifibrotic compounds have been investigated to check their *in vitro* and *in vivo* therapeutic effects on liver cirrhosis.[6,7] For example, interferon-α 2a has been developed for the treatment of hepatitis C virus, one of the main causes of liver cirrhosis. To improve the stability in the body, interferon-α 2a was conjugated with a synthetic polymer of poly(ethylene glycol) [PEG], which was successfully commercialized under the trade name of PEGASYS. However, PEGylation is intended not for targeted delivery to the liver, but for passing through the liver and long circulation in the body. At this viewpoint, PEGylation might not be a good strategy for the development

of liver disease therapeutic delivery systems. Thus, we decided to assess HA derivatives as alternative target-specific drug delivery carriers to the liver in liver disease model mice.
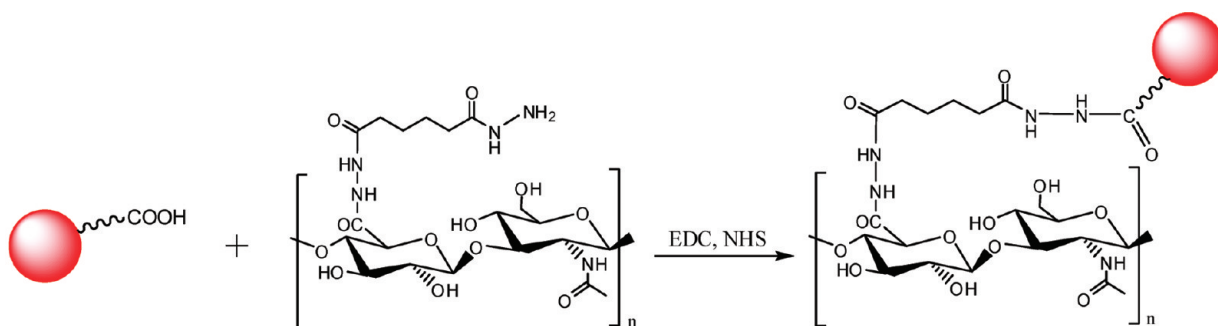
HA is a biodegradable, biocompatible, nonimmunogenic, ubiquitous, and linear polysaccharide with a wide molecular weight (MW) range from 1000 to 10000000 Da.[8] The homeostasis of HA in the body is maintained by HA receptor-mediated degradation in the lymphatics, lymph nodes, blood, liver, and kidney.[9,10] There are many kinds of HA receptors such as cluster determinant 44 (CD44),[11] receptor for hyaluronate-mediated motility (RHAMM),[12,13] HA receptor for endocytosis (HARE),[14,15] and lymphatic vessel endothelial hyaluronan receptor-1 (LYVE-1)[16] with

ABSTRACT Liver fibrosis or cirrhosis is one of the representative liver diseases with a high morbidity and mortality worldwide. Over the past decades, many kinds of antifibrotic compounds have been investigated *in vitro* and *in vivo* for the treatment of liver cirrhosis. In this work, real-time bioimaging of hyaluronic acid (HA) derivatives was carried out using quantum dots (QDots) to assess the possibility of HA derivatives as target-specific drug delivery carriers for the treatment of liver diseases. HA-QDot conjugates with an HA modification degree of about 22 mol % was synthesized by amide bond formation between carboxyl groups of QDots and amine groups of adipic acid dihydrazide modified HA (HA-ADH). According to *in vitro* cell culture tests, HA-QDot conjugates were taken up more to the cells causing chronic liver diseases such as hepatic stellate cells (HSC-T6) and hepatoma cells (HepG2) than normal hepatocytes (FL83B). After tail-vein injection, HA-QDot conjugates were target-specific, being delivered to the cirrhotic liver with a slow clearance longer than 8 days. Furthermore, immunofluorescence and flow cytometric analyses of dissected liver tissues revealed the target-specific delivery of HA derivatives to liver sinusoidal endothelial cells (LSEC) and HSC. The results were thought to reflect the feasibility of HA derivatives as novel drug delivery carriers for the treatment of various chronic liver diseases including hepatitis, liver cirrhosis, and liver cancer.

KEYWORDS: hyaluronic acid · quantum dots · bioimaging · liver cirrhosis · targeted delivery

Scheme 1. Schematic representation for the synthesis of a hyaluronic acid−quantum dot (HA-QDot) conjugate using adipic acid dihydrazide-modified HA (HA-ADH).

various biological functions. In the liver, HA is mainly synthesized by the HSC in the sinusoidal area and degrades by the liver sinusoidal endothelial cells (LSEC).[17] It was reported that HA concentration in the serum elevated drastically during liver fibrosis with no clear explanation of the mechanism.[18,19] CD44 expression also increased in the cases of alcoholic liver disease[20] and dimethylnitrosamine-induced liver cirrhosis.[21] HA receptors have been exploited as target sites for HA-based drug delivery systems. The HA-poly-L-lysine (PLL) conjugate was synthesized, targeting HARE of sinusoidal epithelial cells in the liver.[14,15] CD44 was another good target for HA receptor mediated gene and siRNA delivery.[22] Previously, we carried out real-time bioimaging of HA derivatives using quantum dots (QDots) to investigate the effect of chemical modification of HA on the target-specific cellular uptake by HA receptor mediated endocytosis and the distribution in the body.[23−25] *In vitro* bioimaging study including competitive cellular uptake tests in the presence of free HA confirmed the target-specific delivery of HA derivatives to the cells with HA receptors by HA receptor mediated endocytosis. In addition, HA derivatives with a degree of HA modification less than 25 mol % were mainly accumulated in the liver, whereas highly modified HA derivatives were distributed evenly in the body.[23−25] QDots are semiconductor nanocrystals resistant to photobleaching with a size-tunable photoluminescence, a broad absorption, and sharp emission spectrum.[26] QDots have been extensively studied in the field of molecular bioimaging, because the possibility of their use as a probe for biotagging was reported.[27] Recently, QDots with near-infrared emission wavelengths have attracted a great interest in *in vivo* applications. Near-infrared light has a high penetration depth of about 5−6 cm in the body as compared to that of about 7−10 mm by visible light.[28] Autofluorescence is minimized in the range of near-infrared wavelength contributing to high resolution and accurate quantification.

In this work, real-time bioimaging of HA derivatives was carried out using QDots with a near-infrared emission wavelength of 800 nm to investigate the distribution of HA-QDot conjugates in liver disease model mice. HA-QDot conjugates with an HA modification degree

of about 22 mol % were synthesized by amide bond formation between carboxyl groups of QDots and amine groups of adipic acid dihydrazide modified HA (HA-ADH). On the other hand, a murine model of liver fibrosis was prepared by the treatment with carbon tetrachloride (CCl_4). It is a well-established and valuable animal model to study the biochemical, pathophysiological, and molecular alternations associated with the development of human hepatic fibrosis. The HA-QDot conjugates were applied to the real-time bioimaging of HA derivatives in normal and cirrhotic mice. Conventionally, the bioimaging for temporal evolution of HA derivatives has been monitored only by the sequential sacrifice of many animals. This study demonstrates a long-term, real-time monitoring of HA-QDot conjugates in the body without sacrificing normal and liver fibrosis Balb/c mice. The target-specific delivery of HA derivatives to the liver was discussed for their drug delivery applications to the treatment of liver diseases.

RESULTS AND DISCUSSION

HA derivatives have been widely used as novel drug carriers for target-specific and long-acting delivery of chemical drugs, such as paclitaxel[29] and doxorubicin,[30] and biopharmaceuticals like protein, peptide, and nucleotide therapeutics.[25,31] HA derivatives were developed in the forms of long-acting conjugates, controlled-release microparticles, and selectively cross-linked hydrogels for drug delivery applications.[32,33] In this work, real-time bioimaging of HA-QDot conjugates was carried out to assess the feasibility of HA derivatives as novel target-specific drug delivery carriers for the treatment of liver diseases, especially liver cirrhosis. As shown in Scheme 1, HA-ADH with an ADH content of 22 mol % was conjugated with QDots via amide bond formation between amine groups of HA-ADH and carboxyl groups of QDots using EDC and NHS chemistry. The HA-QDot conjugate had a mean particle size of 42.3 nm and a surface charge of −21.3 mV. The detailed characterization of HA-QDot conjugates is available elsewhere.[23,24,34] The receptor-mediated endocytosis of HA-QDot conjugates was investigated to the normal primary hepatocytes (FL83B), liver disease model cells of hepatic stellate cells (HSC-T6), and

(a)

FL83B   HSC-T6   HepG2

(b)
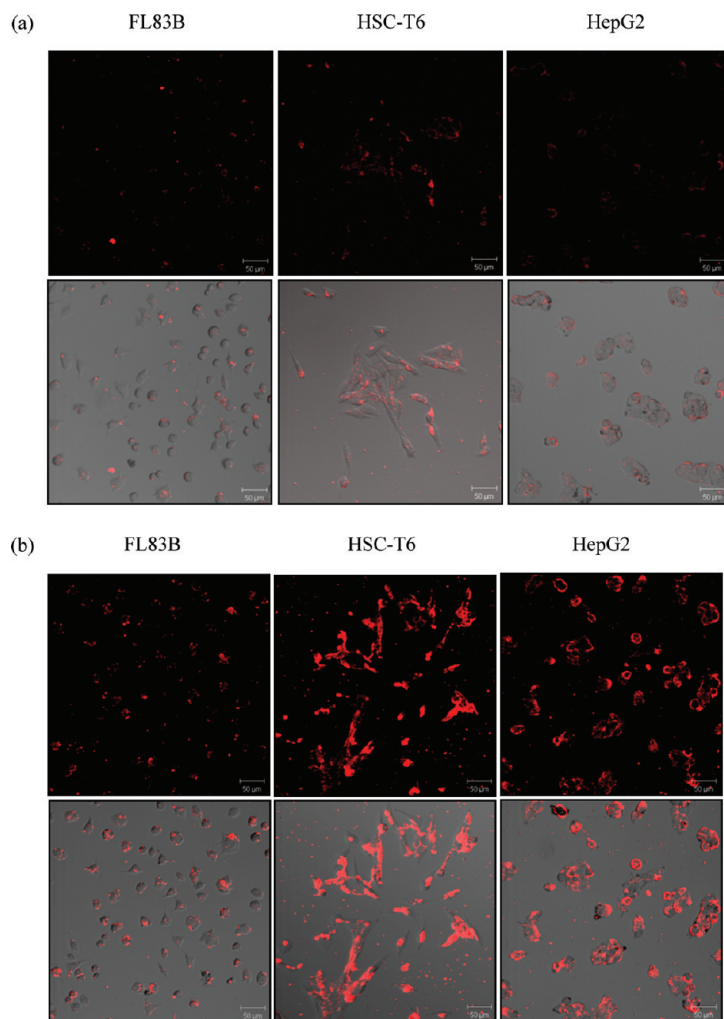
FL83B   HSC-T6   HepG2

Figure 1. Confocal microscopic images of normal hepatocytes (FL83B), hepatic stellate cells (HSC-T6), and hepatoma cells (HepG2) incubated for 2 h with (a) quantum dots (QDots) and (b) hyaluronic acid (HA)−QDot conjugates with 22 mol % HA modification. Scale bar corresponds to 50 μm.

hepatoma cells (HepG2). Figure 1 shows confocal microscopic images of three liver cells (HepG2, HSC-T6, and FL83B) after incubation with QDots and HA-QDot conjugates. HA-QDot conjugates with an ADH content of 22 mol % were thought not to be affected by the binding with HA receptors on the basis of the fact that three carboxyl groups (hexasaccharide) in the HA molecule are related with its binding to HA receptors.[16,35] In accordance with our previous results, HA-QDot conjugates were up-taken to the liver cells with HA receptors more efficiently than QDots alone by the receptor-mediated endocytosis (Figure 1).[23] Interestingly, a larger amount of HA-QDot conjugates could be taken up to liver cancer cells and fibrosis-related cells than normal hepatocytes. The results suggested that liver injury had some physiological effect on the receptor-mediated endocytosis of HA derivatives. Although it was not easy to explain the results clearly, the phenomena reminded us of the enhanced permeation and retention (EPR) effect in cancer cells reflecting the possibility of HA derivatives as novel target-specific drug delivery carriers for the treatment of liver diseases.

On the basis of an *in vitro* bioimaging study, we carried out *in vivo* real-time bioimaging of HA-QDot conjugates in normal and cirrhotic model mice. The cirrhotic mice could be prepared by intraperitoneal injection of CCl_4 twice a week for 8 weeks (Figure 2a). As shown in Figure 2b, inflammatory cells infiltrated around the portal tracts in the livers of mice treated with CCl_4 for 8 weeks. Mononuclear cells representing the infiltrating cell lines were more prevalent in the livers of CCl_4-induced cirrhotic mice than normal mice. In addition to the inflammatory changes, liver fibrosis was confirmed by the nodules and bridging fibrosis in the CCl_4-induced cirrhotic mice. These results were confirmed more clearly by histological analysis of dissected liver tissues after Hematoxylin and Eosin (H&E) and Masson's trichrome stainings (Figure 3). The liver sections of normal control mice showed a negligible amount of ECM and collagen, whereas the CCl_4-treated livers exhibited a remarkable increase in ECM content with bundles of collagen surrounding the lobules. There were large fibrous septa and distorted tissue architectures in the cirrhotic livers (Figure 3).
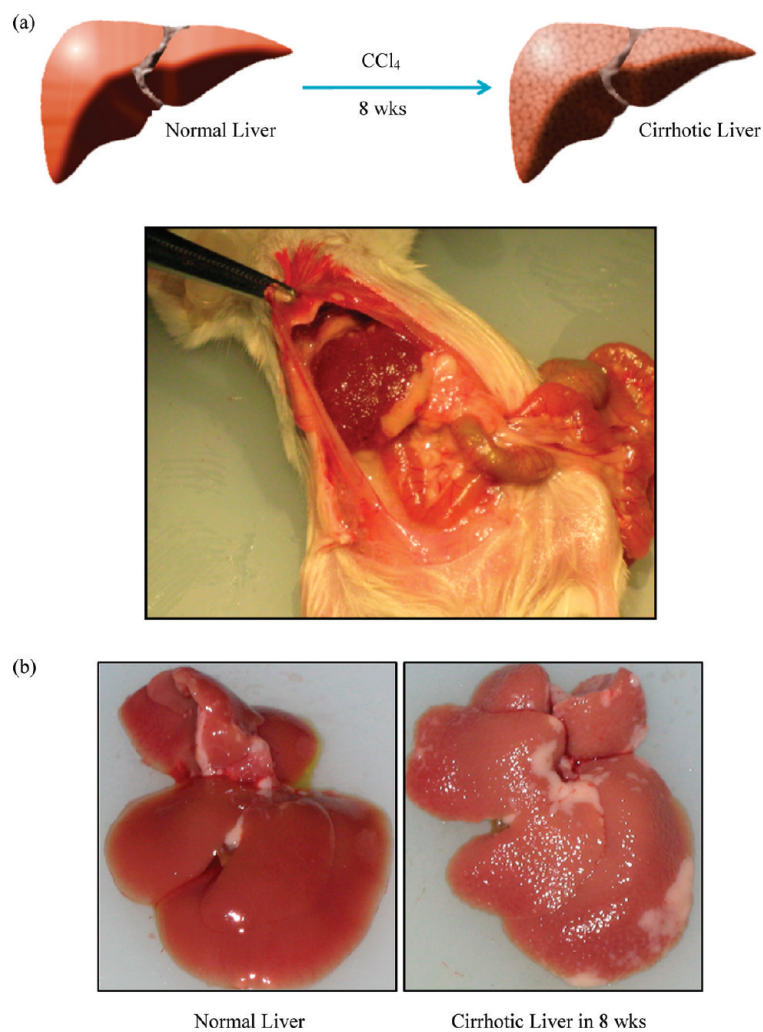
(a)

(b)

Figure 2. (a) Schematic representation for the preparation of cirrhotic model liver and the photograph of a sacrificed cirrhotic mouse. (b) Photographs of normal and cirrhotic livers after treatment with CCl₄ for 8 weeks.

Figure 4 shows the fluorescent images of HA-QDot conjugates after tail-vein injections to normal and fibrotic Balb/c mice. In both cases, HA-QDot conjugates were accumulated mainly in the liver with a similar ini-
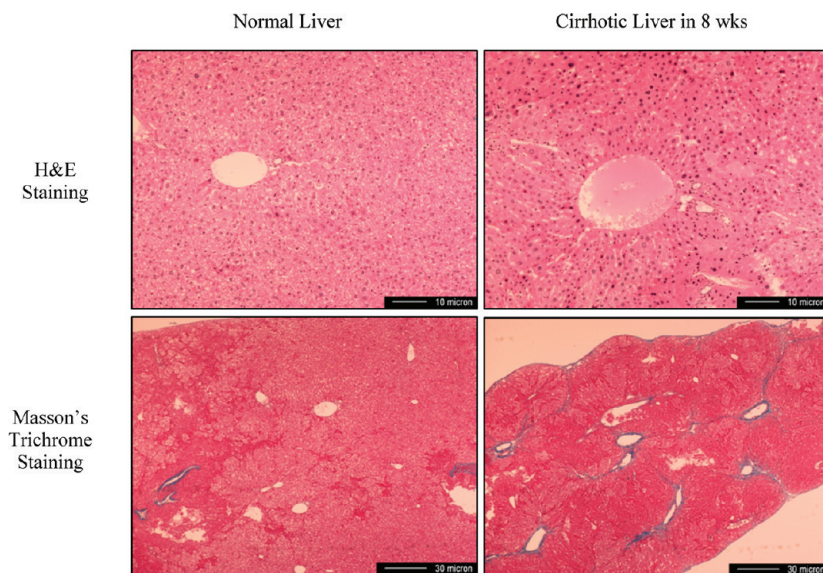

Figure 3. Histological images of normal and cirrhotic livers after Hematoxylin and Eosin (H&E) and Masson's trichrome stainings.
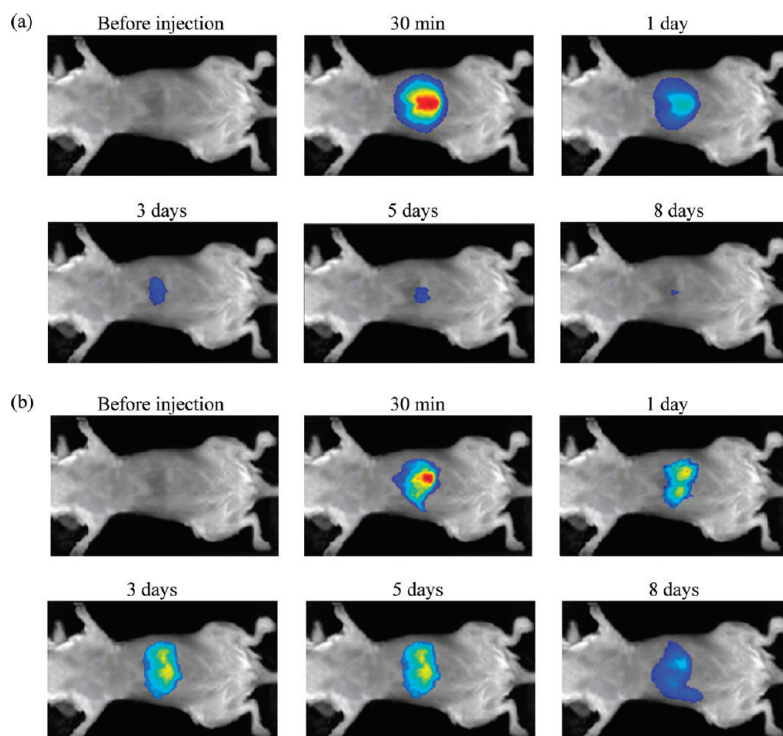
Figure 4. Fluorescent images of the livers in (a) normal and (b) cirrhotic mice with intensity-weighted colors up to 8 days after tail-vein injections of hyaluronic acid−quantum dot (HA-QDot) conjugates.

tial fluorescence intensity. Compared to the normal mice, however, the clearance of HA-QDot conjugates was relatively slow in a cirrhotic liver, remaining even after 8 days. The results may be explained by the assumption that the fibrotic liver becomes lethargic and unable to remove HA-QDot conjugates efficiently (Figure 4). The relative fluorescent intensity was quantified by the region-of-interest (ROI) method, as shown in Figure 5. While the fluorescence intensity of HA-QDot conjugates drastically decreased in the normal livers within 3 days, the fluorescence intensity was maintained in the

range from about 7×10^6 to 10×10^6 RLU in the cirrhotic livers up to 5 days. Statistical analysis revealed the significant difference of fluorescence intensity between normal and cirrhotic livers in 3 days ($P < 0.01$). To make it clear, normal and cirrhotic mice were sacrificed for anatomic analysis 3 days after tail-vein injection of HA-QDot conjugates. Figure 6a shows autoexposed images of dissected liver, spleen, and kidney, and Figure 6b does fluorescent images of the dissected organs. From the results, we could confirm that the fluorescent intensity of HA-QDot conjugates was maintained
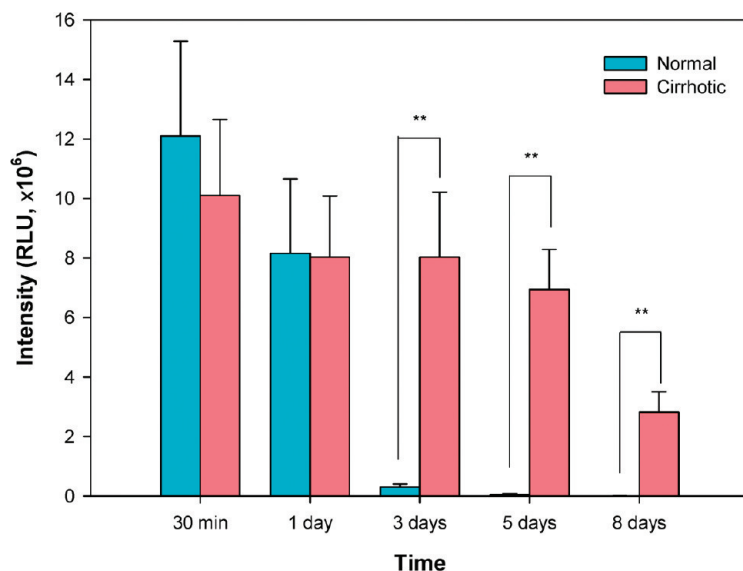

Figure 5. Relative fluorescent intensity of hyaluronic acid−quantum dot (HA-QDot) conjugates in normal and cirrhotic livers up to 8 days after tail-vein injections of HA-QDot conjugates ($P < 0.01$ compared to the normal livers).**
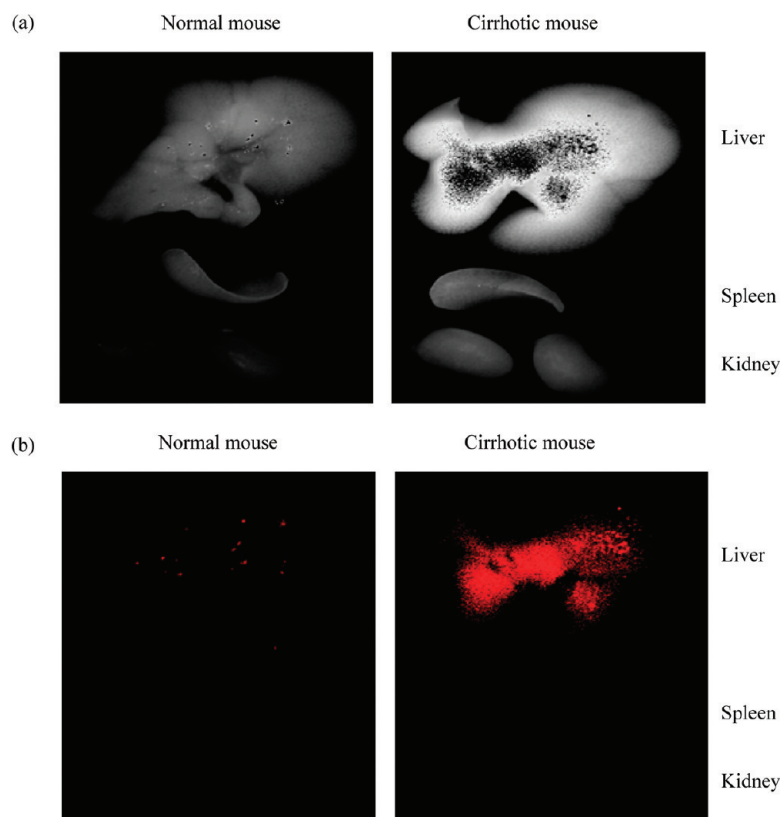
Figure 6. (a) Autoexpose fluorescent images of dissected livers (top), spleens (middle), and kidneys (bottom) 3 days after tail-vein injections of hyaluronic acid - quantum dot (HA-QDot) conjugates to normal and cirrhotic mice. (b) Fluorescent images of (a) at a detection wavelength of 790 nm.

in cirrhotic liver even after 3 days being much stronger than those in the spleen and kidney of cirrhotic mice. In normal mice, however, the fluorescence of HA-QDot conjugates was negligible, reflecting the clearance through reticuloendothelial systems of liver, spleen, and kidney in 3 days.

To investigate the hepatocellular distribution of HA-QDot conjugates in normal and cirrhotic mice, immunofluorescence staining on liver sections was carried out to label biomarkers of LSEC (CD146) and HSC (Desmin).[36] As shown in Figure 7, HA-QDot conjugates were mainly accumulated in LSEC. The fluorescence of HA-QDot conjugates and immunostained CD146 was overlapped each other reflecting the cellular uptake of HA-QDot conjugates to LSEC in both normal and cirrhotic livers (Figure 7a). However, HA-QDot conjugates were predominantly taken up to HSC of cirrhotic liver than normal liver (Figure 7b). The distribution of HA-QDot conjugates in the liver was quantified by flow cytometric analysis. For the case of normal liver, the distribution of HA-QDot conjugates was 70.6% in LSEC, 14% in HSC, and 15.4% in other cells, respectively (Figure 8). In contrast, for the case of cirrhotic liver, the distribution of HA-QDot conjugates was 65% in LSEC, 33.2% in HSC, and 1.8% in other cells, respectively (Figure 8). The quantitative analysis result by flow cytometry was well matched with that of immunofluorescence double

staining analysis. The frequency of HA-QDot positive HSC in the cirrhotic liver was significantly higher than that in the normal liver ($P < 0.01$). Nonparenchymal cells like LSEC and HSC play important roles in the inflammation process of the liver.[37,38] Because HSC exists under the LSEC layer in a normal liver, HSC has a less contacting chance with HA in the blood. However, the more cirrhosis is progressed, the more HSCs are activated. In cirrhotic liver, HSC was reported to be proliferated by $10-20$ times and squeezed through the LSEC fenestrations.[39] All these results suggest that HA derivatives can be applied as novel, target-specific, drug delivery carriers to the treatment of liver cirrhosis.

Although the mechanism is different, the effective cellular uptake and slow clearance of HA-QDot conjugates in cirrhotic livers were thought to be similar with EPR effect in cancer cells. The EPR effect is the property by which certain sizes of molecules, especially in the range of $30-200$ nm, tend to accumulate in tumor tissues much more than they do in normal tissues.[40,41] The blood vessel around the tumor tissue has a leakage structure, making possible the enhanced permeation. The concentration of hyaluronidase is known to be higher around the tissues with tumor and inflammation than normal tissues.[42] In addition, there are several kinds of HA receptors such as CD44 and HARE in the liver as well as in tumor tissue. Considering all these
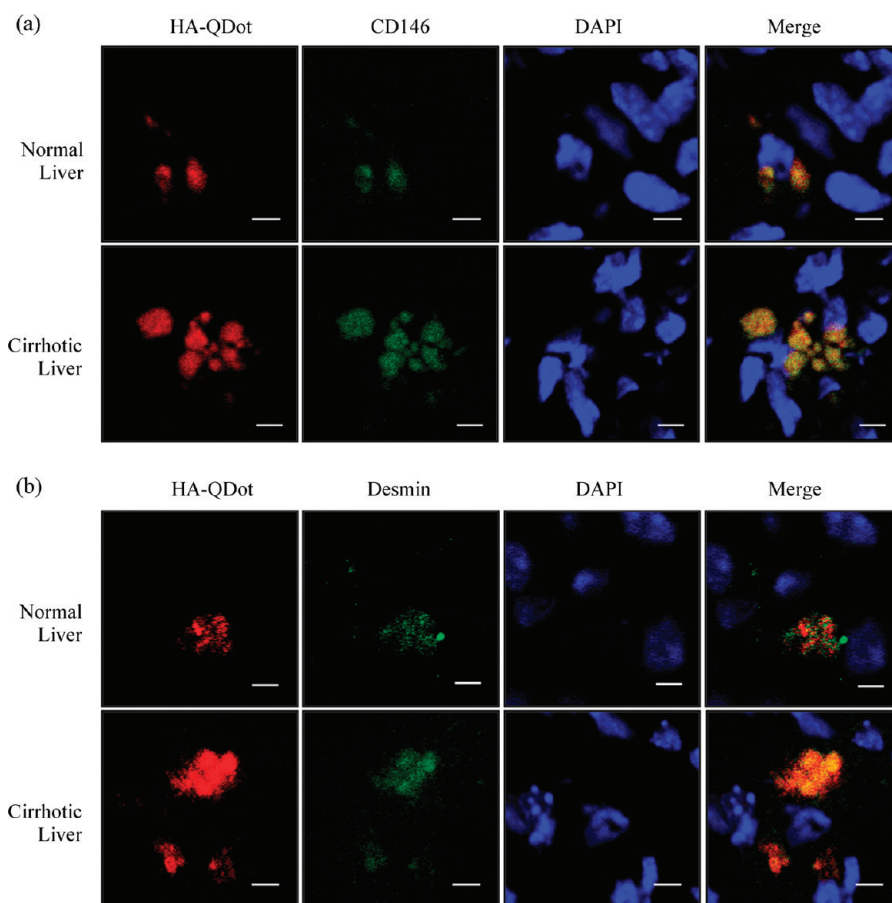
Figure 7. Confocal laser-scanning micrographs showing the immunolocalization of hyaluronic acid−quantum dot (HA-QDot) conjugates in normal and cirrhotic mice. (a) Double staining of liver sinusoidal endothelial cell (LSEC) markers (CD146) and HA-QDot conjugates. (b) Double staining of hepatic stellate cell (HSC) markers (Desmin) and HA-QDot conjugates. Scale bar corresponds to 5 μm.

aspects, the real-time *in vitro* and *in vivo* bioimaging results were thought to be quite reasonable. In a word, HA derivatives appeared to be target-specific, being delivered specifically to the liver, especially to the cirrhotic liver. Currently, we are trying to develop the HA−Interferon-α 2a conjugate as an alternative to PEGASYS, with an increased therapeutic efficacy for the treatment of hepatitis C virus (HCV). According to the phase III clinical test results, the patient rate with a sustained virologic response was only 39% after treatment with PEGASYS.[43] Nowadays, a combination therapy using PEGASYS and Ribavirine is used with a success rate of 57% in patients with HCV genotype 1. The low efficacy may be attributed to the fact that PEGylation is not effective for targeted delivery to the liver but for passing through the liver and long circulation in the body. The low binding affinity to the liver might be advantageous for long circulation, but results in low therapeutic efficacy in the treatment of liver diseases. To the contrary, HA derivatives can be optimized for target-specific and long-acting delivery of various chemical and biopharmaceutical drugs by changing the degree of HA modification.[23,24] As is well-known, HA and chemically modified HA derivatives have been

widely used for various medical applications, demonstrating the safety of HA derivatives with various kinds of functional moieties.[22−25,29−33] HA derivatives will be
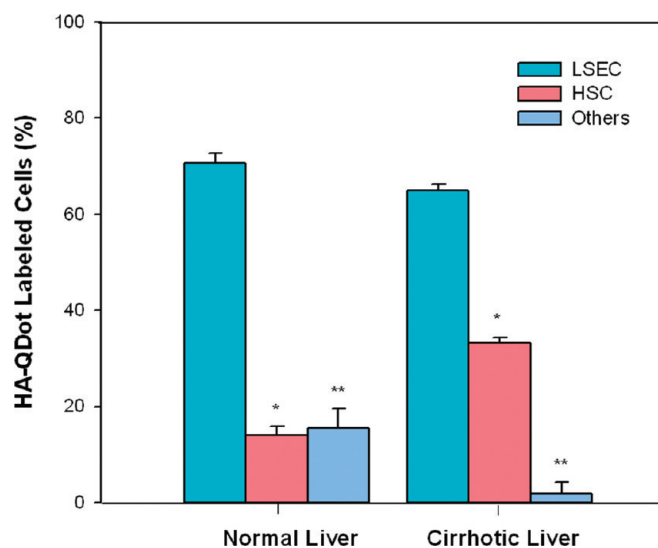

Figure 8. Quantitative analysis of the hepatocellular distribution of hyaluronic acid−quantum dot (HA-QDot) conjugates in normal and cirrhotic mice by flow cytometric analysis (*$P < 0.05$ and **$P < 0.01$ compared to LSEC).

investigated further as novel target-specific and long-acting drug delivery carriers for the treatment of various chronic liver diseases.

CONCLUSION

Real-time bioimaging of HA derivatives was successfully carried out using QDots to assess the feasibility of HA derivatives as target-specific drug delivery carriers for the treatment of liver diseases. HA-QDot conjugates with an HA modification degree of about 22 mol % were synthesized by amide bond formation between carboxyl groups of QDots and amine groups of HA-ADH. *In vitro* cell culture tests showed that HA-QDot conjugates were endocytosed more to the cells, causing chronic liver diseases such as hepatic stellate cells and hepatoma cells than normal hepatocytes. Furthermore, HA-QDot conjugates were delivered in a target-specific manner and accumulated more efficiently in the cirrhotic liver than the normal liver after tail-vein injection. The clearance of HA-QDot conjugates was relatively slow in the cirrhotic liver remaining even after 8 days. In addition, the immunofluorescence and flow cytometric analyses of dissected liver tissues confirmed the target-specific delivery of HA derivatives to LSEC and HSC. All these results demonstrated the feasibility of HA derivatives as novel target-specific and long-acting delivery carriers of chemical and biopharmaceutical drugs for the treatment of various chronic liver diseases, including chronic hepatitis, liver cirrhosis, and liver cancer.

MATERIALS AND METHODS

Materials. Hyaluronic Acid (HA) was purchased from Lifecore (Chaska, MN). *N*-Hydroxysulfosuccinimide (sulfo-NHS), carbon tetrachloride (CCl_4), 4′,6-diamidino-2-phenylindole (DAPI), and Hematoxylin and Eosin (H&E) and Masson's trichrome staining reagents were obtained from Sigma-Aldrich (St. Louis, MO). Quantum dots (QDots) with an emission wavelength of 800 nm were purchased from Invitrogen (Carlsbad, CA), and adipic acid dihydrazide (ADH) and 1-ethyl-3-(3-dimethylaminopropyl)-carbodiimide hydrochloride (EDC) were purchased from Tokyo Chemical Industry (Tokyo, Japan). Fluorescein isothiocyanate (FITC)-labeled mouse anti-CD146 was purchased from Miltenyi Biotech (Gladbach, Germany) and mouse anti-Desmin from Abcam (Cambridge, U.K.). OCT tissue-freezing medium was obtained from Tissuetek (Elkhart, IN), and Alexa 488-labeled anti-mouse IgG was obtained from Jackson Lab (Bar Harbor, ME). Balb/c mice were purchased from Orient Bio Inc. (Seoul, Korea). Ketamine and xylazine (rompun hydrochloride) were obtained from Yuhan Inc. (Seoul, Korea) and Bayer (Seoul, Korea), respectively. HepG2 and FL83B cells were obtained from American Type Culture Collection (Manassas, VA), and an immortalized rat hepatic stellate cell line of HSC-T6 was kindly provided by Prof. SL Friedman (Columbia University, NY).

Synthesis of HA-QDot Conjugates. HA-ADH and HA-QDot conjugates were synthesized as described elsewhere except for a slight modification in the reaction buffer and EDC deactivation method.[33,34] In brief, HA-ADH (3.5 mg) with an ADH content of 22 mol % was dissolved in 1.5 mL of phosphate buffer (0.1 M, pH 5 6.4). QDots (50 μL, *ca.* 0.4 nmol) were mixed with EDC hydrochloride (0.1 mg) and sulfo-NHS (0.3 mg) dissolved in 10 μL of borate buffer. The solution was mixed for 30 min to modify the carboxyl ligands of QDots with sulfo-NHS. Then, 1.4 μL of 2-mercaptoethanol was added to quench the remaining EDC. After mixing for 5 min, 1.5 mL of the HA-ADH solution was added to the activated QDot solution, which was stirred for 2 h. The final solution was buffer-changed with PD-10 column and filtered through 0.2 μm PVDF syringe filter. The resulting HA-QDot conjugates were stored in a refrigerator before use.

In Vitro Bioimaging. HepG2, HSC-T6, and FL83B cells were incubated at 37 °C and 5% CO_2 in DMEM with 10 vol % FBS and 1 wt % antibiotics. Cells were seeded on a 6-well culture dish at a density of 3×10^4 cells/well and incubated in the medium for a day. Then, the culture medium was replaced with DMEM containing 1 vol % FBS. After that, HA-QDot conjugates in 100 μL of DMEM were added to the wells of culture slides. The final concentration of HA-QDot conjugates was 5 nM.[23] The cells were incubated for 2 h, washed with PBS, fixed with 4 wt % paraformaldehyde in PBS, washed again with PBS two times, and observed with a confocal scanning microscope (LSM 510 META, Carl Zeiss, Germany) at a magnification of ×400. The internalized HA-QDot conjugates in the cytoplasm were excited with an Ar laser at 532 nm, and the fluorescence inside the cells was visualized through a long-pass emission filter (650 nm cutoff). As a control, QDots at a concentration of 5 nM were also used for the *in vitro* bioimaging.

Animal Model of Liver Cirrhosis. Six-week-old female Balb/c mice were fed with standard mouse chow (SLC Inc., Shizuoka, Japan) and water *ad libitum*. The animals were housed in an air-conditioned room at 22 ± 1 °C prior to the experiment. All experimental procedures were examined and approved by the Animal Research Ethics Committee at the Catholic University of Korea. Hepatic fibrosis was induced by intraperitoneal administration of CCl_4 dissolved in olive oil (1/9 ratio) at a dose of 0.5 mL/kg body weight twice a week for 8 weeks. The mice were sacrificed at 8 weeks from the first injection of CCl_4. Liver tissues were either snap-frozen in liquid nitrogen or fixed in 10 vol % formalin for histology and immunostaining.

Evaluation of Hepatic Fibrosis. The progression of hepatic fibrosis was analyzed after H&E and Masson's trichrome stainings. Serial sections were stained and examined with a photomicroscope (Olympus Corporation, Tokyo, Japan).

In Vivo Bioimaging. Normal and CCl_4-induced liver cirrhotic mice were anesthetized *via* intraperitoneal injection of a combination of ketamine (100 mg/kg) and xylazine (10 mg/kg). During *in vivo* experiments, the mice were kept under anesthesia and the body temperature was maintained at 37~38 °C. HA-QDot conjugates were administered to CCl_4-induced cirrhotic mice at an average age of 8 weeks by tail-vein injections. The fluorescence of injected HA-QDot conjugates was captured with a luminescent image analyzer (Maestro 2.8, CRI, MA) in 30 min, 1, 3, 5, and 8 days. As a control, the normal mice were also injected with the same molar amount of HA-QDot conjugates intravenously. After 3 days, both mice were sacrificed for the bioimaging of their livers, spleens, and kidneys with the image analyzer. A halogen lamp with a 625 nm filter was used for the excitation, and the fluorescence images were obtained through a 790 nm emission filter.

Immunofluorescence Staining. The distribution of HA-QDot conjugates in liver tissues was investigated by immunofluorescence staining of LSEC and HSC. HA-QDot conjugates were injected intravenously to CCl_4-induced cirrhotic mice. After 12 h, the animals were sacrificed and dissected tissues were mounted on tissue chucks with OCT tissue-freezing medium. Then, the chucks were mounted on a cryostat microtome (Reichert/Jung, Heidelberg, Germany) kept at −80 °C. Sections 4 μm thick were made through the middle of the tissue sample. Frozen sections were stored at −80 °C until needed. Sections were air-dried, fixed in methanol/acetone at 4 °C, washed in PBS for 10 min twice, and permeabilized by incubating with 0.5 wt % Triton X-100 in PBS at room temperature for 3 min. For labeling, sections were washed with PBS twice and blocked with 2 wt % BSA at room temperature for 1 h, followed by the incubation with primary antibody diluted in PBS at 4 °C overnight. Sections were washed in PBS for

10 min 3 times and incubated with Alexa 488-labeled anti-mouse IgG (1:500) at room temperature for 1 h, followed by washing in PBS 3 times. Tissue sections were stained with DAPI to counterstain the nuclei and examined with the confocal scanning microscope. The following primary antibodies were used: FITC-conjugated mouse anti-CD146 (1/1000) and mouse anti-Desmin (1/2000).

Isolation of Hepatic Nonparenchymal Cells and Flow Cytometry. Hepatic nonparenchymal cells (LSEC and HSC) were isolated from the liver of normal and CCl_4-induced cirrhotic mice by the collagenase perfusion two-step method, as described elsewhere.[44] Under ether anesthesia, a midline incision was made in the abdomen of the mice. The portal vein was cannulated with a cut-down tube. The liver was perfused *in situ* with Ca^{2+}-free Hanks' balanced salt (HBS) buffer containing 0.2 vol % ethylene glycol tetraacetic acid and subsequently with HBS buffer containing 1.3 mM $CaCl_2$, 0.015 wt % collagenase, and 0.001 wt % DNase at 37 °C. Immediately after the excision, the liver was minced and suspended in HBS solution containing 0.005 wt % collagenase and 0.001 wt % DNase, and then filtered through a mesh. The cell suspension was centrifuged at $50 \times g$ for 2 min. The supernatant, rich in nonparenchymal cells, was subsequently resuspended after centrifugation at $400 \times g$ and 4 °C for 10 min. Right after the isolation, cell viability was estimated by measuring the number of cells excluding trypan blue. After washing, the isolated cells were resuspended in staining medium of PBS supplemented with 2 vol % fetal bovine serum and 1 wt % antibiotics and then incubated with FITC-conjugated mouse anti-CD146 and mouse anti-Desmin at 4 °C for 30 min. Desmin-stained cells were incubated with antimouse AlexaFluor 488 antibody for 30 min. The cells were washed with staining medium twice prior to the analysis with FACS Calibur flow cytometer (BD Biosciences, San Jose, CA).

Statistical Analysis. The data are presented as mean ± SD. The statistical significance was determined using student's *t*-test and analysis of variance (ANOVA). A value of *P* less than 0.05 was considered statistically significant.

REFERENCES AND NOTES

1. Fontana, R. J.; Goodman, Z. D.; Dienstag, J. L.; Bonkovsky, H. L.; Naishadham, D.; Sterling, R. K.; Su, G. L.; Ghosh, M.; Wright, E. C. HALT-C Trial Group, Relationship of Serum Fibrosis Markers with Liver Fibrosis Stage and Collagen Content in Patients with Advanced Chronic Hepatitis C. *Hepatology* **2008**, *47*, 789–798.

2. Engström-Laurent, A.; Lööf, L.; Nyberg, A.; Schröder, T. Increased Serum Levels of Hyaluronate in Liver Disease. *Hepatology* **1985**, *5*, 638–642.

3. Gabrielli, G. B.; Capra, F.; Casaril, M.; Squarzoni, S.; Tognella, P.; Dagradi, R.; De Maria, E.; Colombari, R.; Corrocher, R.; De Sandre, G. Serum Laminin and Type III Procollagen in Chronic Hepatitis C. Diagnostic Value in the Assessment of Disease Activity and Fibrosis. *Clin. Chim. Acta* **1997**, *265*, 21–31.

4. Ryhanen, L.; Stenback, F.; Ala-Kokko, L.; Savolainen, E. R. The Effect of Malotilate on Type III and Type IV Collagen, Laminin and Fibronectin Metabolism in Dimethylnitrosamine-Induced Liver Fibrosis in the Rat. *J. Hepatol.* **1996**, *24*, 238–245.

5. Friedman, S. L. Seminars in Medicine of the Beth Israel Hospital, Boston. The Cellular Basis of Hepatic Fibrosis. Mechanisms and Treatment Strategies. *N. Engl. J. Med.* **1993**, *328*, 1828–1835.

6. Hui, A. Y.; Friedman, S. L. Molecular Basis of Hepatic Fibrosis. *Expert Rev. Mol. Med.* **2003**, *5*, 1–23.

7. Schuppan, D.; Popov, Y. Hepatic Fibrosis: From Bench to Bedside. *J. Gastroenterol. Hepatol.* **2002**, *17* (Suppl 3), S300–305.

8. Kuo, J. W. *Practical Aspects of Hyaluronan Based Medical Products*; Taylor & Francis: New York, 2006.

9. Prevo, R.; Banerji, S.; Ferguson, D. J.; Clasper, S.; Jackson, D. G. Mouse LYVE-1 is an Endocytic Receptor for Hyaluronan in Lymphatic Endothelium. *J. Biol. Chem.* **2001**, *276*, 19420–19430.

10. Stern, R.; Asari, A. A.; Sugahara, K. N. Hyaluronan Fragments: An Information-Rich System. *Eur. J. Cell Biol.* **2006**, *85*, 699–715.

11. Aruffo, A.; Stamenkovic, I.; Melnick, M.; Underhill, C. B.; Seed, B. CD44 is the Principal Cell Surface Receptor for Hyaluronate. *Cell* **1990**, *61*, 1303–1313.

12. Entwistle, J.; Hall, C. L.; Turley, E. A. HA Receptors: Regulators of Signalling to the Cytoskeleton. *J. Cell. Biochem.* **1996**, *61*, 569–577.

13. Toole, B. P. *Hyaluronan-Cell Interactions in Morphogenesis*; Portland Press: London, 1998.

14. Asayama, S.; Nogawa, M.; Takei, Y.; Akaike, T.; Maruyama, A. Synthesis of Novel Polyampholyte Comb-Type Copolymers Consisting of a Poly(L-lysine) Backbone and Hyaluronic Acid Side Chains for a DNA Carrier. *Bioconjugate Chem.* **1998**, *9*, 476–481.

15. Takei, Y.; Maruyama, A.; Ferdous, A.; Nishimura, Y.; Kawano, S.; Ikejima, K.; Okumura, S.; Asayama, S.; Nogawa, M.; Hashimoto, M.; Makino, Y.; Kinoshita, M.; Watanabe, S.; Akaike, T.; Lemasters, J. J.; Sato, N. Targeted Gene Delivery to Sinusoidal Endothelial Cells: DNA Nanoassociate Bearing Hyaluronan-Glycocalyx. *FASEB J.* **2004**, *18*, 699–701.

16. Schledzewski, K.; Falkowski, M.; Moldenhauer, G.; Metharom, P.; Kzhyshkowska, J.; Ganss, R.; Demory, A.; Falkowska-Hansen, B.; Kurzen, H.; Ugurel, S.; Geginat, G.; Arnold, B.; Goerdt, S. Lymphatic Endothelium-Specific Hyaluronan Receptor LYVE-1 is Expressed by Stabilin-1+, F4/80+, CD11b+ Macrophages in Malignant Tumours and Wound Healing Tissue. *In Vivo* and in Bone Marrow Cultures *In Vitro*: Implications for the Assessment of Lymphangiogenesis. *J. Pathol.* **2006**, *209*, 67–77.

17. Eriksson, S.; Fraser, J. R.; Laurent, T. C.; Pertoft, H.; Smedsrod, B. Endothelial Cells are a Site of Uptake and Degradation of Hyaluronic Acid in the Liver. *Exp. Cell Res.* **1983**, *144*, 223–228.

18. Guechot, J.; Loria, A.; Serfaty, L.; Giral, P.; Giboudeau, J.; Poupon, R. Serum Hyaluronan as a Marker of Liver Fibrosis in Chronic Viral Hepatitis C: Effect of α-Interferon Therapy. *J. Hepatol.* **1995**, *22*, 22–26.

19. Oberti, F.; Valsesia, E.; Pilette, C.; Rousselet, M. C.; Bedossa, P.; Aube, C.; Gallois, Y.; Rifflet, H.; Maiga, M. Y.; Penneau-Fontbonne, D.; Cales, P. Noninvasive Diagnosis of Hepatic Fibrosis or Cirrhosis. *Gastroenterology* **1997**, *113*, 1609–1616.

20. Urashima, S.; Tsutsumi, M.; Ozaki, K.; Tsuchishima, M.; Shimanaka, K.; Ueshima, Y.; Takase, S. Immunohistochemical Study of Hyaluronate Receptor (CD44) in Alcoholic Liver Disease. *Alcohol.: Clin. Exp. Res.* **2000**, *24*, 34S–38S.

21. Satoh, T.; Ichida, T.; Matsuda, Y.; Sugiyama, M.; Yonekura, K.; Ishikawa, T.; Asakura, H. Interaction between Hyaluronan and CD44 in the Development of Dimethylnitrosamine-Induced Liver Cirrhosis. *J. Gastroenterol. Hepatol.* **2000**, *15*, 402–411.

22. Lee, H.; Mok, H.; Lee, S.; Oh, Y. K.; Park, T. G. Target-Specific Intracellular Delivery of siRNA Using Degradable Hyaluronic Acid Nanogels. *J. Controlled Release* **2007**, *119*, 245–252.

23. Jiang, G.; Park, K.; Kim, J.; Kim, K. S.; Hahn, S. K. Target Specific Intracellular Delivery of siRNA/PEI-HA Complex by Receptor Mediated Endocytosis. *Mol. Pharm.* **2009**, *6*, 727–737.

24. Kim, J.; Kim, K. S.; Jiang, G.; Kang, H.; Kim, S.; Kim, B. S.;

Park, M. H.; Hahn, S. K. *In Vivo* Real-Time Bioimaging of Hyaluronic Acid Derivatives Using Quantum Dots. *Biopolymers* **2008**, *89*, 1144–1153.

25. Oh, E. J.; Park, K. T.; Kim, K. S.; Kim, J. S.; Yang, J. A.; Kong, J. H.; Lee, M. Y.; Hoffman, A. S.; Hahn, S. K. Target Specific and Long-Acting Delivery of Protein, Peptide, and Nucleotide Therapeutics Using Hyaluronic Acid Derivatives. *J. Controlled Release* **2010**, *141*, 2–12.

26. Michalet, X.; Pinaud, F. F.; Bentolila, L. A.; Tsay, J. M.; Doose, S.; Li, J. J.; Sundaresan, G.; Wu, A. M.; Gambhir, S. S.; Weiss, S. Quantum Dots for Live Cells, *In Vivo* Imaging, and Diagnostics. *Science* **2005**, *307*, 538–544.

27. Chan, W. C.; Nie, S. Quantum Dot Bioconjugates for Ultrasensitive Nonisotopic Detection. *Science* **1998**, *281*, 2016–2018.

28. Weissleder, R.; Tung, C. H.; Mahmood, U.; Bogdanov, A., Jr. *In Vivo* Imaging of Tumors with Protease-Activated Near-Infrared Fluorescent Probes. *Nat. Biotechnol.* **1999**, *17*, 375–378.

29. Luo, Y.; Ziebell, M. R.; Prestwich, G. D. A Hyaluronic Acid-Taxol Antitumor Bioconjugate Targeted to Cancer Cells. *Biomacromolecules* **2000**, *1*, 208–218.

30. Luo, Y.; Bernshaw, N. J.; Lu, Z. R.; Kopecek, J.; Prestwich, G. D. Targeted Delivery of Doxorubicin by HPMA Copolymer-Hyaluronan Bioconjugates. *Pharm. Res.* **2002**, *19*, 396–402.

31. Oh, E. J.; Kim, J. W.; Kong, J. H.; Ryu, S. H.; Hahn, S. K. Signal Transduction of Hyaluronic Acid-Peptide Conjugate for Formyl Peptide Receptor like 1 Receptor. *Bioconjugate Chem.* **2008**, *19*, 2401–2408.

32. Kim, S. J.; Hahn, S. K.; Kim, M. J.; Kim, D. H.; Lee, Y. P. Development of a Novel Sustained Release Formulation of Recombinant Human Growth Hormone Using Sodium Hyaluronate Microparticles. *J. Controlled Release* **2005**, *104*, 323–335.

33. Motokawa, K.; Hahn, S. K.; Nakamura, T.; Miyamoto, H.; Shimoboji, T. Selectively Crosslinked Hyaluronic Acid Hydrogels for Sustained Release Formulation of Erythropoietin. *J. Biomed. Mater. Res. A* **2006**, *78*, 459–465.

34. Kim, J.; Park, K.; Hahn, S. K. Effect of Hyaluronic Acid Molecular Weight on the Morphology of Quantum Dot-Hyaluronic Acid Conjugates. *Int. J. Biol. Macromol.* **2008**, *42*, 41–45.

35. Banerji, S.; Wright, A. J.; Noble, M.; Mahoney, D. J.; Campbell, I. D.; Day, A. J.; Jackson, D. G. Structures of the CD44-Hyaluronan Complex Provide Insight into a Fundamental Carbohydrate−Protein Interaction. *Nat. Struct. Mol. Biol.* **2007**, *14*, 234–239.

36. Mochizuki, S.; Kano, A.; Shimada, N.; Maruyama, A. Uptake of Enzymatically Digested Hyaluronan by Liver Endothelial Cells *In Vivo* and *In Vitro*. *J. Biomater. Sci., Polym. Ed.* **2009**, *20*, 83–97.

37. Edwards, M. J.; Keller, B. J.; Kauffman, F. C.; Thurman, R. G. The Involvement of Kupffer Cells in Carbon Tetrachloride Toxicity. *Toxicol. Appl. Pharmacol.* **1993**, *119*, 275–279.

38. Rieder, H.; Armbrust, T.; Meyer zum Buschenfelde, K. H.; Ramadori, G. Contribution of Sinusoidal Endothelial Liver Cells to Liver Fibrosis: Expression of Transforming Growth Factor-β 1 Receptors and Modulation of Plasmin-Generating Enzymes by Transforming Growth Factor-β 1. *Hepatology* **1993**, *18*, 937–944.

39. Warren, A.; Bertolino, P.; Benseler, V.; Fraser, R.; McCaughan, G. W.; Le Couteur, D. G. Marked Changes of the Hepatic Sinusoid in a Transgenic Mouse Model of Acute Immune-Mediated Hepatitis. *J. Hepatol.* **2007**, *46*, 239–246.

40. Matsumura, Y.; Maeda, H. A New Concept for Macromolecular Therapeutics in Cancer Chemotherapy: Mechanism of Tumoritropic Accumulation of Proteins and the Antitumor Agent Smancs. *Cancer Res.* **1986**, *46*, 6387–6392.

41. Vasey, P. A.; Kaye, S. B.; Morrison, R.; Twelves, C.; Wilson, P.; Duncan, R.; Thomson, A. H.; Murray, L. S.; Hilditch, T. E.; Murray, T.; Burtles, S.; Fraier, D.; Frigerio, E.; Cassidy, J. Phase I Clinical and Pharmacokinetic Study of PK1 [*N*-(2-Hydroxypropyl)methacrylamide Copolymer Doxorubicin]: First Member of a New Class of Chemotherapeutic Agents−Drug−Polymer Conjugates. Cancer Research Campaign Phase I/II Committee. *Clin. Cancer Res.* **1999**, *5*, 83–94.

42. Lee, H.; Lee, K.; Kim, I. K.; Park, T. G. Synthesis, Characterization, and *In Vivo* Diagnostic Applications of Hyaluronic Acid Immobilized Gold Nanoprobes. *Biomaterials* **2008**, *29*, 4709–4718.

43. Knäblein, J., Ed. In *Modern Biopharmaceuticals*; Wiley-VCH: Weinheim, Germany, 2005; Supplementary CD-ROM.

44. Friedman, S. Isolation and Culture of Hepatic Nonparenchymal Cells. In *In Vitro Biological Systems*; Tyson, C., Frazier, J., Eds.; Academic Press: San Diego, CA, 1993; Vol. 1, p 292310.